Article

Not peer-reviewed version

Evaluation of the mineral manganese OXMN009 and OXMN009P in the Chemical looping Combustion (CLC) process using Thermogravimetry

Sandra Peña *, Carmen Forero, Francisco Velasco-Sarria, Eduardo Arango

Posted Date: 24 June 2024

doi: 10.20944/preprints202406.1571.v1

Keywords: solid oxygen transporter; manganese oxide; chemical looping combustion.

 doi:10.20944/preprints202406.1571.v1

Article

Evaluation of the Mineral Manganese OXMN009 and OXMN009P in the Chemical Looping Combustion (CLC) Process Using Thermogravimetry

Sandra Peña [1,*], Carmen Forero [2], Francisco Velasco-Sarria [2] and Eduardo Arango [2]

[1] University of Guayaquil
[2] University of Valle; carmen.forero@correounivalle.edu.co; francisco.velasco@correounivalle.edu.co; eduardo.arango@correounivalle.edu.co
* Correspondence: sandra.penam@ug.edu.ec; Tel.: +593999630391 SEPM

Abstract: Carbon dioxide capture chemical looping combustion (CLC) technology uses metal oxides as oxygen transporters (TO). (1) These oxygen transporters, OXMN009 and OXMN009P, are used in a cyclic process that prevents the formation of nitrogen oxides by keeping air and fuel separate. (2) Thermogravimetric balance (TGA) experiments were conducted to evaluate the kinetic behavior of these copper-modified oxygen transporters. (3) It was found that OXMN009P has improved reactivity and oxygen transfer properties due to copper impregnation. The kinetic parameters obtained in the TGA indicate that the reaction is non-thermal and requires less energy to initiate. (4) The results show that OXMN009P has reactivity comparable to other manganese-based materials reported in the literature and can be an effective option for carbon dioxide capture.

Keywords: solid oxygen transporter; manganese oxide; chemical looping combustion

1. Introduction

The CLC process is a flexible and versatile technology that can be used with a wide range of fuels, both gaseous (methane, syngas, etc.); liquids (ethane, diesel, etc.), and solids (coal and biomass); In addition, this process is based on the transfer of oxygen from air to fuel through a solid oxygen carrier, usually a metal oxide. This conveyor constantly circulates between two interconnected fluidized bed reactors, known as a reduction reactor (RR) and an oxidation reactor (RO). This arrangement prevents direct contact between fuel and air throughout the combustion process [1].

Compared to conventional fossil fuel combustion technologies, the CLC process has the potential to significantly reduce greenhouse gas emissions and improve air quality. Figure 1.

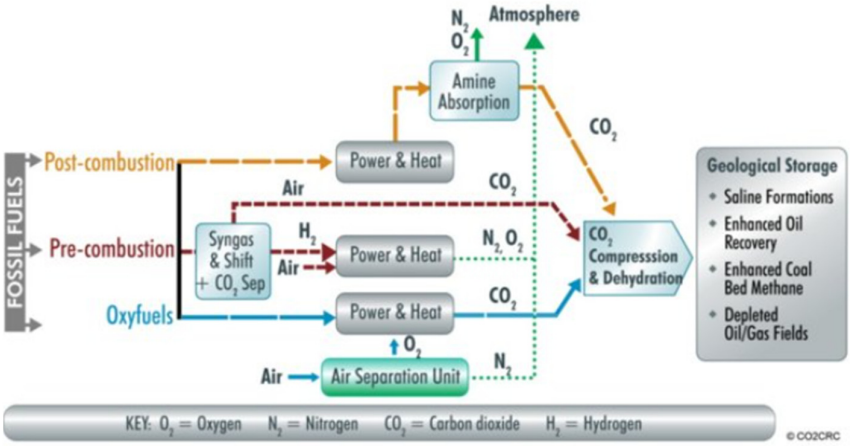

 doi:10.20944/preprints202406.1571.v1

Figure 1. Post-combustion capture, carbon utilization, and storage technologies.

CLC relies on the transfer of oxygen from air to fuel via an oxygen transporter to prevent contact between air and fuel.

Oxygen transport is achieved by continuously circulating the oxygen transporter between two interconnected fluidized bed reactors (fuel and air reactors). In fuel reactors, fuel is oxidized to carbon dioxide (CO_2) and water vapor (H_2O) primarily through the reduction of metal oxides.

The reduced oxygen carrier is then sent to an air reactor where it is re-oxidized with the oxygen in the air. The combustion of coal and other solid fuels using CLC technology can be achieved through three processes: ex-situ combustion through gasification chemical cycle (iG-CLC), in-situ gasification chemical combustion (iG-CLC), and chemical cycle decoupling oxygen (CLOU) [2].

2. Materials and Methods

New methods and protocols should be described in detail while well-established methods can be briefly described and approved Combustion with solid oxygen carriers (CLC) is the most suitable technology for CO_2 capture. The main function of these systems is to separate the CO_2 produced into a gas stream with a high CO_2 concentration.

There is a variety of referenced literature, with the difference of TSO preparation methods, among them are: mechanical mixing [3], coprecipitation [4,5], mediated synthesis of surfactant [6,7], granulation by freezing [8–10] and impregnation [11,12]. The TSO particles used in these methods have a porous structure with a large surface area, facilitating the diffusion of reaction gases to metal oxide. But, any study in the preparation of large-scale TSO is novel to science [10].

Given the high cost of producing synthetic TSOs, low-cost OTs, such as ilmenite, manganese, and iron ores, are sought. Like iron, manganese metal oxides are becoming increasingly important because they are cheap and non-toxic and have higher transport capacity compared to iron.

The highest oxidation state of Mn is MnO_2, which decomposes at 500°C. However, at temperatures above 800 °C, only Mn_3O_4 is a stable material. For this reason, only the conversion between Mn_3O_4 and MnO is considered for its application in CLC. Mn_2O_3 can be used as an alternative to the CLOU process.

Recently, a large number of studies have been carried out on materials formed by the mixture of manganese oxides, which have shown good suitability to be used in the process [13–15]; However, in this type of material, the decoupling of oxygen is highly conditioned by the conditions required for its previous oxidation. In addition, these solids have always been characterized by their low mechanical resistance, which has not allowed more than 4 hours of combustion with gases in a unit in continuous compound stirring. Evidently, this aspect has been an important conditioning factor in obtaining a manganese-based conveyor, not only for the coal removal process but for the process in general [3]. Therefore, in this research, an oxygen transporter based on this oxide was developed that had improved characteristics that allowed to increase the combustion efficiency using thermogravimetry. For this, it was necessary to propose and develop the selection of the most suitable material for the prepared solid, based on the positive variables (oxygen transport capacity, mechanical resistance, and reaction speed) that have been reported with excellent results, as indicated in Equation (1).

Identifying solid compounds that have the ability to transfer oxygen in the CLC system is essential. Therefore, a compound must have a high conversion of fuel to CO_2 and H_2O. Jerndal et al., 2006 presented an extensive thermodynamic analysis of several systems considered CLC. It recorded oxides of Cu, Ni, Co, Fe, and Mn with favorable thermodynamics to react with CH_4, H_2, and CO, with equilibrium constant at the temperatures and pressures required in CLC [16,17].

2.1. Preparation of Materials

From the project "Combustion with CO_2 capture by means of solid oxygen transporters (Chemical Looping Combustion)" with the aim of finding potential low-cost TSOs in the country, 16 natural minerals from different regions were characterized by X-ray fluorescence analysis (XRF),

 doi:10.20944/preprints202406.1571.v1

including OXMN009, from these data there is a resistance to rupture 5.7 and they were tested in a TGA using CH_4, CO andH_2 as fuel. To achieve the required particle size, the mill with blade attachment was used and the ground sample was passed through a sieve no.70 (Tyler series), which guaranteed a diameter between 100 and 300 μm.

The screening and sufficiency process of the size of the manganese-based oxygen transporter was carried out; then calcination was performed on the 0XMN009 solid conveyor, to increase its mechanical strength and obtain a modified manganese 0XMN009P; in the incipient impregnation method for Cu processing of the selected sample, adding a 5 M solution volume of copper nitrate trihydrate ($Cu(NO_3)_2.3H_2O$) corresponding to the pore volume of the material, which allowed contact between the ore and the impregnant, then the copper nitrate was decomposed into copper oxide, the sample was calcined at a temperature of 550 °C and finally a second calcination was performed at 850 °C to stabilize the sample.

Available materials (original and modified solid oxygen carriers) were characterized by X-ray fluorescence (XRF) to quantify the concentration of manganese-based materials, followed by thermogravimetric analysis. SEM (Scanning Electron Microscopy) characterization and X-ray diffraction (XRD) were performed to identify the crystalline phases present in oxygen-carrying particles.

For TSO's XRF analysis, a PANalytical AXIOS max sequential wavelength dispersive X-ray fluorescence spectrometer (WDXRF) was used equipped with a rhodium tube with a maximum power of 4.0 KW. It uses a primary hybrid monochromator that produces a parallel beam, ideal for studying grazing samples (thin layers) to quantify elements present in the sample; useful for reading diffraction pattern information obtained with XRD.

For the XRD analysis of the TSOs, Panalytical Empyrean equipment with a cobalt X-ray source was used to perform a sweep between the 20° to 100° angles of the 2θθ range to identify the crystalline phases of the materials.

For the SEM analysis, a JEOL-JSM 6490 LV Scanning Electron Microscope was used, which uses electrons instead of light to form the image, to achieve this the device has a filament that generates a beam of electrons to illuminate the sample, and if the sample is not conductive, it must be covered with a thin layer of gold. The images produced by this method can be used to determine the morphology of TSO.

EDS analysis was used for elemental identification by chemical mapping using the same electron microscopy described above, which was useful in identifying Cu deposited in the immersion-treated TSO.

2.2. Thermogravimetric Balance Analysis

The assembly and commissioning of the thermogravimetric analysis (TGA) system for the CLC process was carried out. TGA analysis was performed on the solid oxygen (OXMN009) manganese transporting material with particle diameters D to determine: conversion at four different temperatures (between 650 and 950°C), using CH_4, CO, and H_2 as fuel, where the experimental design is indicated for three factors: CH_4, CO and H_2; therefore, the number of experiments was 24; In addition, the type of material (M1), temperature (Ti), the constant Ci fuel concentration.

TGA CI Electronics

The TGA Cl Electronics monitors the changes in mass that a sample undergoes when exposed to controlled atmospheres for a given period of time. This equipment has an accuracy of 0.1 μm and also offers the possibility of working at high temperatures and with atmospheres of different compositions.

The advantage offered by this equipment is the diversity of working atmospheres, which were CO, CH_4, and H_2, which were needed in the present study. The equipment is composed of a furnace, a data collection system called LabWeight, a reactor, a head that is where the most sensitive part of the equipment is located, the balance, with which the weight variations that the sample undergoes when exposed to the study conditions are determined, valves, meters, controllers, etc. A disbal

 doi:10.20944/preprints202406.1571.v1

system, temperature controller, and a bubbler allow the injection of steam into the reactor **Error! Reference source not found.**.

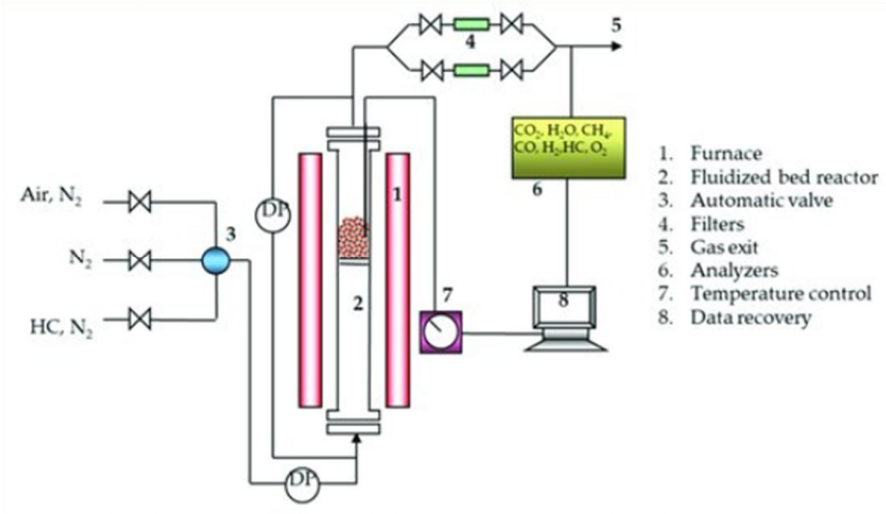

Figure 2. LCC TGA Ci Electronics Schematic.

El método utilizado para el procedimiento de análisis termogravimétrico consistió en agregar 50 mg ± 1 mg de TSO a la canasta, que luego se colocó en un extremo de la TGA y se calentó a la temperatura de trabajo en una atmósfera de aire. Una vez que se alcanza la temperatura de funcionamiento, el TSO mantiene una masa constante y comienza el análisis. El TSO pasa por ciclos de reducción y oxidación, alternando líneas de gas, manteniendo un caudal volumétrico constante de 25 LN/h. El registro obtenido en la termobalanza es: el cambio de peso o pérdida de masa, y el tiempo de la reacción de oxidación o reducción del TO; luego de la purga de N_2 para garantizar un ambiente inerte después de la reducción; dando lugar a la regeneración completa de TO por ganancia de peso en la etapa de oxidación—reducción

3. Results

Among Mn minerals, OXMN09 had the lowest reactivity with CH_4 in TGA, however, in the literature Mattisson, Johansson, & Lyngfelt, (2006) reported that Mn-based TSO had low reactivity with CH_4 and high reactivity with H_2 and CO. Therefore, the material of the present study OXMN009 was brought to a particle size between 100 and 300 μm.

Orrego (2017) investigated the effect of the initial impregnation of Cu in Fe and Mn TSO, the study variables were the type of fuel (CH_4 and H_2) and percentage of Cu impregnated (1.5%, 3.5%, and 5%), found that using H_2 as reducing gas and Cu impregnation percentage between 3.5% and 5%, the improvement in TSO reactivity was more pronounced. For the above reasons, and considering that the detection limit of the XRD equipment used to identify the crystalline phases in the material is 4%, it was decided to impregnate the TSO for this study with 5% Cu.

To obtain OXMN009 with 5 wt.% Cu, the impregnation procedure was carried out, as indicated above, resulting in that, although multiple calculations were required, the particle size remained constant in the TSO, indicating that There was no significant agglomeration of particles when subjected to temperatures up to 1050 °C in an oxidizing atmosphere.

Through the XRF analysis, the characterization of the OXMN009 and OXMN009P materials (93.15% and 89.32%) is reflected, as indicated in Table 1, it was carried out to determine the presence of Mn elements associated with low-cost TO, so the presence of these elements in high concentrations indicates the potential of the mineral as TO [18–21].

 doi:10.20944/preprints202406.1571.v1

Table 1. Xrf Análysis.

Element	Original Element OXMN009	Modified Element OXMN009P
Mg	0.10	0.07
Al	0.36	0.21
Si	3.49	1.88
P	0.13	0.12
Si	0.04	0.01
K	0.07	0.05
Ca	0.17	0.19
Ti	0.02	0.02
V	0.03	0.02
Mn	93.15	89.32
Fe	2.34	1.59
Cu		6.35
Zn	0.02	0.02
As	0.02	0.02

[1] Tables may have a footer.

Samples OXMN009 and OXMN009P have a high Mn content, which makes Mn oxide the main active phase in these materials; the Si content is low, so the presence of mixed oxides of Mn and Si as the active phase is negligible. The presence of a variety of metals in low proportions in XRF analysis is a common characteristic of natural minerals, so to facilitate subsequent calculations, only active phases that can form with most elements are considered.

The results reported in Table 2 correspond to the crystalline phases detected in the diffractograms obtained. The large number of low-intensity peaks found and the overlap of peaks at closed $2\theta\theta$ angles, which usually occurs in natural minerals, indicate that the crystalline phases reported in Table 2 are not all they are likely that there are also unidentified phases. XRD analysis detected thermite (CuO) in the Cu-treated TSO, consistent with an initial impregnation process performed in which the sample was calcined at 850 °C in an oxidizing atmosphere to decompose the added copper nitrate and form copper oxide. copper.

Table 2. Reduction and oxidation reactions of the active phases found in TSO.

Active phase	Stage	Reagent	Reaction
CuO	Reduction	CO	$CuO + CO \rightarrow Cu + CO_2$
		H_2	$CuO + H_2 \rightarrow Cu + H_2O$
	Oxidation	CH_4	$CuO + CH_4 \rightarrow Cu + CO_2 + H_2O$
Mn_3O_4	Reduction	CO	$Mn_3O_4 + CO \rightarrow 3MnO + CO_2$
		H_2	$Mn_3O_4 + H_2 \rightarrow 3MnO + H_2O$
	Oxidation	CH_4	$Mn_3O_4 + CH_4 \rightarrow Mn_3O_4 + CO_2 + H_2O$

Table 3. X-RAY Disfraction.

CRYSTALLINE PHASE			
Name	**Formula**	**OXMN009**	**OXMN009P**
Hausmanite	Mn_3O_4		
Bixbite	MnO_3		X
Quartz	SiO_2	X	X
Theronite	CuO	X	
Hematite	Fe_2O_3		X
Chromite	$FeCr_2O_4$		
Pseudobrookite	Fe_2TiO_5		

 doi:10.20944/preprints202406.1571.v1

In samples OXMN009 and OXMN009P, two oxidation states of manganese oxide were detected: chertolite (Mn_2O_3) and bixbyite (Mn_3O_4). [18,27], studied the reduction and oxidation behavior of Mn oxides and found that once Mn_2O_3 was reduced to Mn_3O_4, its reoxidation was not detectable at high temperatures (800 °C), because on the other hand on the other hand, they found that Mn_3O_4 can be reduced to MnO and is easily reoxidized to Mn_3O_4 in air. Therefore, only the Mn_3O_4/MnO system in CLC is considered [15].

SEM microscopy of TSO was taken in its native state and processed at magnifications of 50, 100, and 3000 to understand the morphology, size distribution, and possible differences caused by Cu treatment. SEM microscopy of samples OXMN009 and OXMN009P are indicated in Table 4. No difference was observed between the two solids at 50x and 100x magnification. Both have irregular size distribution, flat particle shape, and rough surface; At 3000x magnification, a large number of pores can be seen on the surface of sample OXMN009, but in sample OXMN009P these pores appear to be occupied, possibly by impregnated CuO particles.

Table 4. SEM microscopies of samples OXMN009 and OXMN009P at 50, 100, and 3000x magnification.

OXMN009	OXMN009P
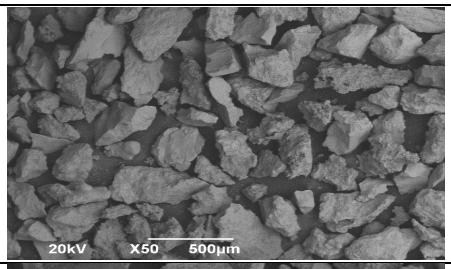	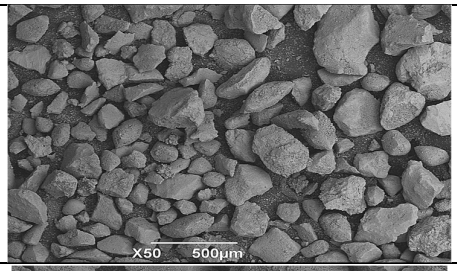
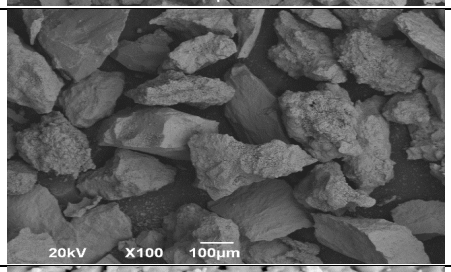	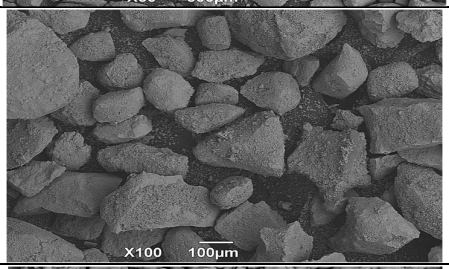
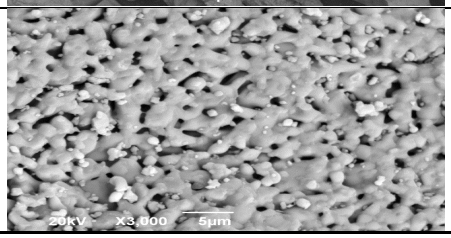	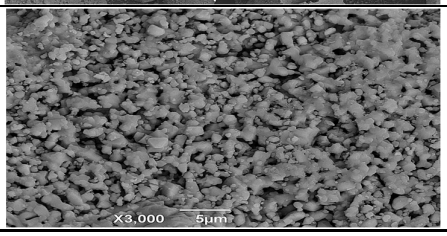

The EDS analysis was performed on the TSOs in their raw and processed states. To create a representative distribution of the elements on the surface of the samples, 9 points were chosen for the detection of dispersive energy in the microscopies at 100x magnification of each of the TSOs (see Table 4). For each solid oxygen carrier, Table 5 lists the elements that were found in their maximum and minimum concentrations.

Table 5. EDS analysis results for TSOs.

		Al	Si	Ti	Cr	Mn	Fe	Cu
OXMN009	Max	3,7	-	-	-	89,7	11,0	-
	Min	1,4	-	-	-	11,1	2,1	-
OXMN009P	Max	2,2	14,9	-	-	78,7	12,3	13,4
	Min	2,2	0,5	-	-	55,6	1,7	2,3

 doi:10.20944/preprints202406.1571.v1

Finding high Mn contents in OXMN009 and OXMN009P, the elemental composition results in Table *5*, support the findings in FRX (see Table 1) and DRX (see Table 2). Cu was discovered in the processed TSO at each elemental detection point, indicating that the element is well distributed within the TSO particles. It should also be noted that the EDS results were only used to determine the presence of the impregnated phase and its distribution in the TSO particles because they do not represent the total elemental composition of the samples.

The TSO OXMN009 and 0XMN009P, under study, were analyzed in TGA, which allowed the determination of the oxygen transport capacities, reaction rate indices, and kinetic parameters for the materials with the best behavior.

To know the effect of copper treatment on the studied TSO, the reduction and oxidation conversion curves of the native and treated TSO obtained under the same operating conditions in TGA were compared. The operating temperature of 950 °C was chosen for these preliminary tests to show agglomeration problems, which did not occur in any of the samples studied. The analysis of the samples in an H_2 atmosphere gave positive results in terms of reactivity, in addition, the samples treated with Cu showed higher reduction and oxidation conversions at 30 seconds. On the other hand, the analysis in a CO atmosphere showed similar results in OXMN009P for the reduction of Mn TSO and greater oxidation conversion at 30 seconds. However, this result is insufficient, since the impregnation of Cu reactivity would have been improved TSO with CO as fuel.

Table 6 shows the Reaction rate indices (*R*I) obtained for the preliminary analyses carried out on each sample, which were calculated according to Equation (1), facilitating the comparison of the reaction rate between different TSOs; indicated in Equation 1, in the conversion delta between 0 and 0.15 when the reaction is faster and the *Pr* was set at 0.15 atm which is commonly used in the literature [8,13]. OXMN009P has a higher *R*I than OXMN009, and both materials present *R*I in the range reported in the literature for other Mn materials (see Table 6).

Table 6. *R*I (%/min) in TGA tests at 950 °C of the Mn minerals reported in the literature.

	***R*I (%/min)**	
Material	**CO**	**H_2**
OXMN009	5,8	15,1
OXMN009P	6,1	20,1
Ilmenita [a 1]	2,5	7,9
Residuo de Bauxita [1]	3,9	10,5
Mineral (hematita) [1]	3,4	12,4
MnSA [2]	5,1(5,3)[a]	14,2 (11,8)
MnGBHNE [2]	6,4 (1,4)	19,2 (9,0)
MnGBMPB [2]	9,0 (2,4)	26,4 (14,8)
MnBR [2]	8,2 (3,0)	20,5 (12,5)
Mineral de Mn [2]	-	19,8 [b]

a ( )Materials used, b averages 900 y 1000oC, 1 [13,25].

The activation energies (Ea) obtained for OXMN009 and OXMN009P using CO, H_2, and CH_4 as reactive gases are between 5 and 18.7 kJ/mol, a similar range to that found in the literature for Mn-based TSO (10, 2 to 19.5 kJ/mol)[22] and lower than that reported for synthetic TSO of Fe, Cu, Ni, and Mn (14 to 33 kJ/mol) [5] and other materials of natural origin such as activated Ilmenite (25.5 to 80.7 kJ/mol) [23]. The Ea reported for OXMN009P are lower than those of OXMN009 in the reduction reactions, indicating that there is less dependence of the reaction on temperature and therefore a lower energy is necessary to trigger the reaction Levenspiel, (1993); However, the oxidation a lower Ea was obtained in OXMN009.

The kinetic parameters (k_0) found for OXMN009 and OXMN009P are of a similar order of magnitude in all the reactions studied and are close to that reported in the literature Zafar, (2007) for the oxidation of MnO to Mn_3O_4 (1.04 m^3 mol 0.65 s^{-1}).

 doi:10.20944/preprints202406.1571.v1

Figure 3 shows that the experimental data fit linearly to the grain SCM model for both OXMN009 and OXMN009P for all gases studied.

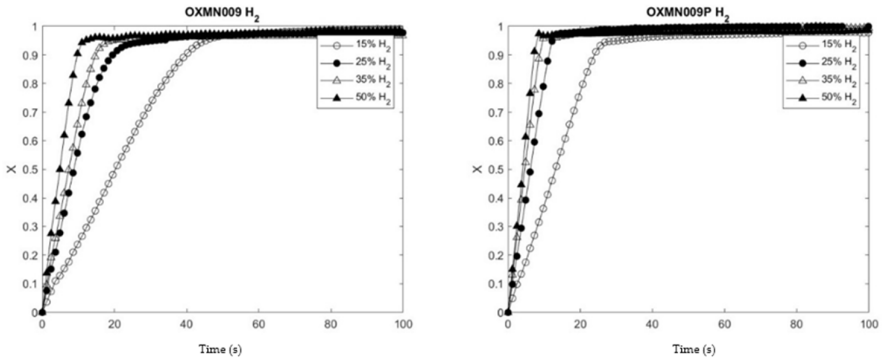

Figure 3. Comparison OXMN009 y OXMN009P. Red: 25% H_2 y 75% N_2; Ox: 100% Aire; T: 950 °C.

The calculated reaction orders of OXMN009 and OXMN009P with CH_4 (0.7; 0.7), H_2 (1.11; 1.09), CO (1.5; 1.0) respectively as shown in Table 8, are within the ranges reported for synthetic Mn with CH_4 (1.0) and O_2 (0.65), and within the ranges reported for synthetic Cu-based minerals with CH_4 (0.4), H_2 (0.6), CO (0.8) and O_2 (1.0); Fe with CH_4 (1.3), H_2 (0.8), CO (1.0) and O_2 (1.0); Nor with CH_4 (0.4), H_2 (0.6), CO (0.8) and O_2 (1.0) [24]. In general, the reaction order also depends on the fuel used. Regarding CH_4, the reaction order obtained presents the same order of magnitude based on what was previously reported by Zafar and collaborators [21]. The results indicate that the reaction rate for the transporters studied follows first-order kinetics on average. The complete conversion times τ found are shown in Table 8. The correlation coefficients obtained from the linear regression X vs. Time are in the range of 0.9594 to 0.9999, reflecting that the conversion varies linearly with time and fits the SCM model proposed following what was stated by Arango, (2016) [15].

Table 7. Reaction Order.

Material	Reactive	n	r^2
OXMN009	H_2	1,1	0,9574
	CH_4	0,7	0,9999
	CO	1,5	0,9999
OXMN009P	H_2	1,0	0,9472
	CH_4	0,7	0,9174
	CO	1,0	0,9990

Table 8. Kinetics of materials 0XMN009 and OXMN009P.

Sample	Fuel	Ea (kJ/mol)	Ko m/s(mol/m³)^n	Order (n)	Temperature °C	Fuel concentration % (v/v)	Oxygen concentration % (v/v)
OXMN009	CH_4	59,38	2,26E+00	0,7	650–950	15–30	21
	H_2	18,74	5,29E-01	1,11	650–950	15–30	21
	CO	23,97	1,38E-01	1,53	650–900	15–30	21
OXMN009P	CH_4	40,49	1,44E+00	0,7	650–950	15–30	21
	H_2	12,09	4,61E-01	0,99	650–950	15–30	21
	CO	11,07	7,96E-02	0,97	650–950	15–30	21

 doi:10.20944/preprints202406.1571.v1

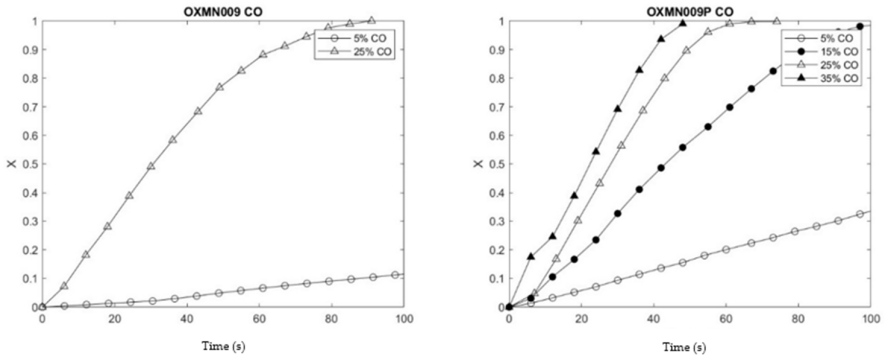

Figure 4. Comparison OXMN009 y OXMN009P. Red: 25%CO y 75% N_2; Ox:100% Air; T: 950 °C.

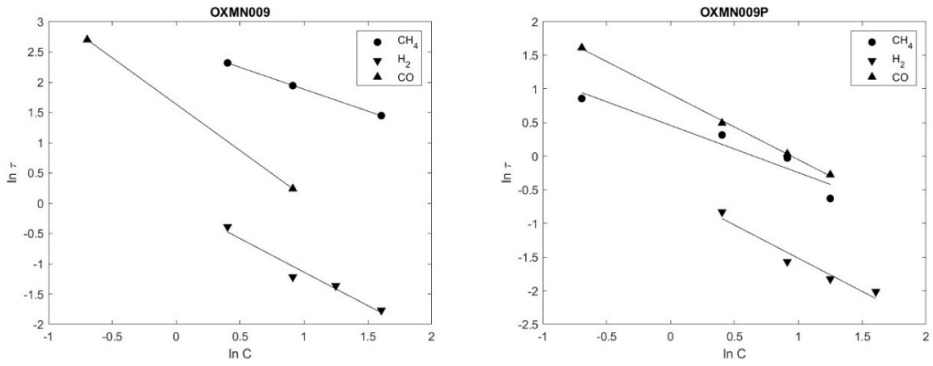

Figure 5. Ln(τ) Vs Ln(C) OXMN009; OXMN009P (Reductor gas: H_2, CO y CH_4 entre 5 %–50%, balance con N_2. Air 100 %. T = 950°C.

Formatting of Mathematical Components

$$RI = 100 * 60 * Ro * \left(\frac{dx}{dt}\right)_{norm} \quad (1)$$

4. Discussion

In this study, a Manganese mineral (OXMN009) was modified with Cu with the incipient impregnation method and related to its use in CLC technology. It was found that OXMN009 in its natural state has a much lower reactivity with CO and H_2 than OXMN009P, and also did not suffer improvements when processed. Based on the above, the research called the mineral (OXMN009) natural state and the mineral (OXMN009P) processed or improved.

5. Conclusions

In this research, the behavior of the minerals OXMN009 and OXMN009P was evaluated in thermogravimetric analyses (TGA) containing CO, H_2, and CH_4, which gave reaction products with RI reaction rates (7.9-20.1%/min) comparable to other manganese-based materials reported in the literature and the reactivity persisted constant during 30 successive redox cycles. In addition, improvements in the reactivity and oxygen transfer properties related to copper impregnation were obtained for the mineral OXMN009P.

For the tests on the thermogravimetric balance (TGA) available in the Fuel Combustion Laboratory of the Universidad del Valle, CO, CH_4, and H_2 fuels were required, and for its operation, the equipment of both the TGA and the LFd were conditioned, with their respective complements.

 doi:10.20944/preprints202406.1571.v1

The TGA products provided the kinetic parameters for the reduction of OXMN009 and OXMN009P (with CO and H_2) with activation energies ranging between 11.0 and 28.0 kJ/mol, demonstrating that the reaction is non-thermal at 650 -950°C. independent and requires less energy to start. The dependence of the studied data on the concentration of the reagent is approx. 1 ± 0.1, which is related to the publications on Mn materials

Supplementary Materials: The following supporting information can be downloaded at: https://ugye-my.sharepoint.com/:f:/g/personal/sandra_penam_ug_edu_ec/EknhTWpSP2RIuU1GOL4eDHYBNBvDWcr0BVYPii_6so5g7Q?e=uzvgY. Figure S1–S3: title; Table S1–S5.

Author Contributions: The Conceptualization and methodology, Sandra Peña; to the validation Eduardo Arango; investigation, resources, Sandra Peña; writing—original draft preparation, Sandra Peña; review Carmen Forero and Francisco Velasco editing; visualization, supervision, project administration, Carmen Forero.

Funding: This research received no external funding.

Institutional Review Board Statement: Not applicable.

Informed Consent Statement: Not applicable for studies not involving humans.

Data Availability Statement: Data Availability Statements are available in section "https://ugye-my.sharepoint.com/:f:/g/personal/sandra_penam_ug_edu_ec/EknhTWpSP2RIuU1GOL4eDHYBNBvDWcr0BVYPii_6so5g7Q?e=uzvgY0" at https://www.ug.edu.ec.

Acknowledgments: The authors gratefully acknowledge the financial support provided by the Colombia Scientific Program within the framework of the call Ecosistema Científico (Contract No. FP44842- 218-2018); and Coal Science and Technology Laboratory of the Universidad del Valle, Cali- Colombia. The gratitude for the support received by the Petroleum Laboratory of the Faculty and Career of Chemical Engineering of the University of Guayaquil, Guayaquil-Ecuador.

Conflicts of Interest: The authors declare no conflict of interest.

References

1. J. Yan and Z. Zhang, "Carbon Capture, Utilization and Storage (CCUS)," *Applied Energy*, vol. 235. pp. 1289–1299, 2019. doi 10.1016/j.apenergy.2018.11.019.
2. A. Cabello, A. Abad, P. Gayán, L. F. De Diego, F. García-Labiano, and J. Adánez, "Effect of operating conditions and H2S presence on the performance of CaMg0.1Mn0.9O3-δ perovskite material in chemical looping combustion (CLC)," *Energy and Fuels*, vol. 28, no. 2, pp. 1262–1274, Feb. 2014, doi: 10.1021/EF4020718.
3. R. Pérez-Vega, A. Abad, P. Gayán, L. F. de Diego, F. García-Labiano, and J. Adánez, "Development of (Mn0.77Fe0.23)2O3 particles as an oxygen carrier for coal combustion with CO2 capture via in-situ gasification chemical looping combustion (iG-CLC) aided by oxygen uncoupling (CLOU)," *Fuel Processing Technology*, vol. 164, pp. 69–79, 2017, doi: 10.1016/j.fuproc.2017.04.019.
4. I. Adánez-Rubio, A. Abad, P. Gayán, L. F. De Diego, F. García-Labiano, and J. Adánez, "Biomass combustion with CO2 capture by chemical looping with oxygen uncoupling (CLOU)," *Fuel Processing Technology*, vol. 124, pp. 104–114, Aug. 2014, doi: 10.1016/J.FUPROC.2014.02.019.
5. J. Adánez, C. Dueso, L. De Diego, F. García-Labiano, P. Gayán, and A. Abad, "Methane combustion in a 500 Wth chemical-looping combustion system using an impregnated ni-based oxygen carrier," *Energy and Fuels*, vol. 23, no. 1, pp. 130–142, Jan. 2009, doi: 10.1021/EF8005146.
6. B. Song and J. A. Forsyth, "Carbon Capture and Hydrogen Production with Membranes," *Energy Procedia*, vol. 37, pp. 1050–1059, Jan. 2013, doi: 10.1016/J.EGYPRO.2013.05.201.
7. C. Xu *et al.*, "Kinetic models comparison for steam gasification of coal/biomass blend chars," *Bioresour Technol*, vol. 171, no. 1, pp. 253–259, 2014, doi: 10.1016/j.biortech.2014.07.099.
8. T. Mattisson, "Materials for Chemical-Looping with Oxygen Uncoupling," *ISRN Chemical Engineering*, vol. 2013, pp. 1–19, May 2013, doi: 10.1155/2013/526375.
9. M. Keller, M. Arjmand, H. Leion, and T. Mattisson, "Interaction of mineral matter of coal with oxygen carriers in chemical-looping combustion (CLC)," *Chemical Engineering Research and Design*, vol. 92, no. 9, pp. 1753–1770, 2014, doi: 10.1016/j.cherd.2013.12.006.

 doi:10.20944/preprints202406.1571.v1

10. C. Linderholm, M. Schmitz, P. Knutsson, and A. Lyngfelt, "Chemical-looping combustion in a 100-kW unit using a mixture of ilmenite and manganese ore as an oxygen carrier," *Fuel*, vol. 166, pp. 533–542, Feb. 2016, doi: 10.1016/j.fuel.2015.11.015.
11. L. F. de Diego, "Estado actual del proceso de combustión con transportadores sólidos de oxígeno : Current status of Chemical Looping Combustion process," *Boletín del Grupo Español del Carbón*, vol. 35, no. 35, pp. 21–25, 2015, [Online]. Available: https://dialnet.unirioja.es/servlet/catart?codigo=5111518
12. E. Arango, C. Forero, and F. Velasco-Sarria, "Use of a Low-Cost Colombian Manganese Mineral as a Solid Oxygen Carrier in Chemical Looping Combustion Technology," *Energy and Fuels*. 2021. doi: 10.1021/acs.energyfuels.1c00587.
13. S. K. Haider *et al.*, "Manganese Minerals as Oxygen Carriers for Chemical Looping Combustion of Coal," *Ind Eng Chem Res*, vol. 55, no. 22, pp. 6539–6546, 2016, doi: 10.1021/acs.iecr.6b00263.
14. E. Arango, "Development of low-cost solid oxygen carriers based on iron and/or manganese available in Colombia using CO and H2 as fuels in clc (chemical looping combustion) technology.," 2013.
15. E. Arango and F. Vasquez, "Determinación de los parámetros cinéticos para la combustión usando minerales del suroccidente colombiano como transportadores sólidos de oxígeno," 2016. Accessed: Sep. 26, 2021. [Online]. Available: https://bibliotecadigital.univalle.edu.co/handle/10893/16893
16. F. Snijkers, E. Jerndal, I. Thijs, T. Mattisson, A. Lyngfelt, and S. Frans, "Preparation of oxygen carriers for chemical looping combustion by industrial spray drying method," *Proc 1st Int Conf on Chemical Looping*, no. March, pp. 1–10, 2010.
17. E. Jerndal, T. Mattisson, and A. Lyngfelt, "Thermal analysis of chemical-looping combustion," *Chemical Engineering Research and Design*, vol. 84, no. 9 A, pp. 795–806, Sep. 2006, doi: 10.1205/cherd05020.
18. I. Adánez-Rubio *et al.*, "Chemical looping combustion of biomass: CLOU experiments with a Cu-Mn mixed oxide," *Fuel Processing Technology*, vol. 172, pp. 179–186, Apr. 2018, doi: 10.1016/j.fuproc.2017.12.010.
19. Abad, Adánez, Forero, Garcia, and Gayán, "Captura de CO2 mediante transportadores sólidos," *Revista Colombiana de Química*, p. 1, 2010.
20. T. Mattisson, A. Lyngfelt, and H. Leion, "Chemical-looping with oxygen uncoupling for combustion of solid fuels," *International Journal of Greenhouse Gas Control*, vol. 3, no. 1, pp. 11–19, 2009, doi: 10.1016/j.ijggc.2008.06.002.
21. Q. Zafar, A. Abad, T. Mattisson, B. Gevert, and M. Strand, "Reduction and oxidation kinetics of Mn3O4/Mg–ZrO2 oxygen carrier particles for chemical-looping combustion," *Chem Eng Sci*, vol. 62, no. 23, pp. 6556–6567, Dec. 2007, doi: 10.1016/J.CES.2007.07.011.
22. F. Velasco-Sarria, C. Forero, I. Adánez-Rubio, A. Abad, and J. Adánez, "Assessment of low-cost oxygen carrier in South-western Colombia, and its use in the in-situ gasification chemical looping combustion technology," *Fuel*, vol. 218, pp. 417–424, Apr. 2018, doi: 10.1016/j.fuel.2017.11.078.
23. C. Forero, J. Adánez, P. Gayán, L. De Diego, G.-L. Francisco, and A. Abad, "CO2 Capture by Chemical Looping Combustion," *Revista Colombiana de Química*, vol. 39, no. 2, pp. 271–285, 2010.
24. A. Abad, P. Gayán, F. García-Labiano, L. F. de Diego, and J. Adánez, "Relevance of plant design on CLC process performance using a Cu-based oxygen carrier," *Fuel Processing Technology*, vol. 171, pp. 78–88, Mar. 2018, doi: 10.1016/j.fuproc.2017.09.015.
25. T. Mendiara, A. Jensen, and P. Glarborg, "Chemical Looping Reforming of Generator Gas," no. February, 2010.